

# Performance of translucent optical networks under dynamic traffic and uncertain physical-layer information<sup>\*</sup>

M. Yannuzzi<sup>1</sup>, M. Quagliotti<sup>2</sup>, G. Maier<sup>3</sup>, E. Marín-Tordera<sup>1</sup>, X. Masip-Bruin<sup>1</sup>, S. Sánchez-López<sup>1</sup>,  
J. Solé-Pareta<sup>1</sup>, W. Erangoli<sup>4</sup>, G. Tamiri<sup>5</sup>

<sup>1</sup>Technical University of Catalonia (Spain), <sup>2</sup>Telecom Italia (Italy), <sup>3</sup>Politecnico di Milano (Italy)  
<sup>4</sup>Pirelli Labs (Italy), <sup>5</sup>CoreCom (Italy)

**Abstract**— This paper investigates the performance of translucent Optical Transport Networks (OTNs) under different traffic and knowledge conditions, varying from perfect knowledge to drifts and uncertainties in the physical-layer parameters. Our focus is on the regular operation of a translucent OTN, i.e., after the dimensioning and regenerator placement phase. Our contributions can be summarized as follows. Based on the computation of the Personick’s  $Q$  factor, we introduce a new methodology for the assessment of the optical signal quality along a path, and show its application on a realistic example. We analyze the performance of both deterministic and predictive RWA techniques integrating this signal quality factor  $Q$  in the lightpath computation process. Our results confirm the effectiveness of predictive techniques to deal with the typical drifts and uncertainties in the physical-layer parameters, in contrast to the superior efficacy of deterministic approaches in case of perfect knowledge. Conversely to most previous works, where all wavelengths are assumed to have the same characteristics, we examine the case when the network is not perfectly compensated, so the Maximum Transmission Distance (MTD) of the different wavelength channels may vary. We show that blocking might increase dramatically when the MTD of the different wavelength channels is overlooked.

## I. INTRODUCTION

In transparent Optical Transport Networks (OTNs), the optical signal from a source to a destination is handled entirely in the optical domain—meaning that Optical-Electrical-Optical (O-E-O) conversions are never performed at transit nodes. Full transparency, however, is not always achievable in long distance networks due to physical impairments (both linear [1] and non-linear [2]) that degrade the Optical Signal-to-Noise Ratio (OSNR) as optical signals propagate transparently through the network. When the impairments accumulated along a route are excessively high, lightpaths cannot be established, so connection requests are blocked. This is because it cannot be guaranteed that the signal detection at destination occurs with a Bit Error Rate (BER) lower than a certain threshold. In order to geographically expand a transparent OTN, an operator might need to install one or more regenerators along some paths, so as to provide sufficient end-to-end quality to optical connections. Clearly, regenerators break up the optical continuity, but allow improving the OSNR—hence

reducing the BER. The deployment of regenerators turns a transparent OTN into a translucent network.

During the dimensioning of an OTN, the Routing and Wavelength Assignment and Regenerator Placement (RWARP) process requires an effective method for estimating the potential degradation of an optical signal along the candidate paths, which is typically achieved by integrating physical-layer information into the RWARP process. Once the regenerators are placed and the dimensioning phase has concluded, the role of the RWA process is to route the forecasted traffic demands according to the planning. Unfortunately, the stochastic nature of traffic demands, the fact that the network might not be perfectly compensated, together with the uncertainties and drifts of the physical-layer parameters from their nominal values during the operation of the OTN, lead to situations where the performance achieved by the RWA process is significantly worse than projected.

In this context, the contribution of this work is twofold. First, we propose a straightforward methodology—based on the computation of the Personick’s  $Q$  factor—for estimating the quality of an optical signal along a transparent sub-path, i.e., the segment of a lightpath comprised between two regenerators. Second, we investigate the performance of deterministic and predictive RWA techniques that integrate this signal quality factor  $Q$  in the lightpath computation process. Their performance is analyzed under different limited-knowledge conditions: (i) dynamic traffic demands; (ii) uncertainty about the values of the physical-layer parameters affecting the computation of the  $Q$  factor; and (iii) possibility of imperfect compensation of the OTN. Our results show that whereas deterministic RWA strategies are effective under a perfect knowledge condition, they can be substantially improved by predictive techniques in the more realistic case where uncertainties arise during the regular operation of the OTN. We also provide insight into the potential consequences of overlooking the wavelength selection when the OTN is not perfectly compensated and/or equalized. In particular, our results reveal that for an uncompensated OTN, the blocking might increase dramatically when the maximum reachable distance by the different wavelength channels is disregarded.

## II. THE TRANSLUCENT OTN MODEL

The OTN model that we consider is composed by the following elements: translucent optical nodes, regenerators,

<sup>\*</sup> The work was carried out with the support of the BONE-project (“Building the Future Optical Network in Europe”), a Network of Excellence funded by the European Commission through the 7th ICT-Framework Programme and the FP6 EC NOBEL2 IP, the FP7 EC DICONET, and the National Spanish project TEC2008-02552-E.

transponders, and DWDM line systems. A translucent node is composed of an all-optical switching fabric that is able to switch an optical signal from an input port to an output port without electrical processing. We assume that nodes are supported by a non-blocking switching fabric, which only introduces attenuation. The input/output ports of the node (the tributaries) are connected to tunable transponders that provide the appropriate color (wavelength) and power level to the optical signal (see Fig.1). We consider that transit signals are not directly processed by regenerators and/or converters located at the network ports, but rather, a pool of regenerators/converters can be connected at dedicated ports of the switching fabric to flexibly allow regeneration and wavelength conversion (shown at the bottom of Fig. 1). The number of such regenerators is determined by the RWARP process during the dimensioning phase. The regeneration of a bidirectional WDM channel crossing a node requires four unidirectional (or two bidirectional) node ports and one (bidirectional) regenerator. We consider 3R regenerators, which make an O-E-O conversion providing the three digital regeneration functions of: re-amplification, re-shaping and re-timing. After a transit signal has been processed by a 3R regenerator, it regains the physical features it had at the source node, i.e., at the output of the tributary transponder that was used to inject the signal into the network. Thus, from a signal-impairment point of view, a regeneration operation implies a complete loss of memory of the history of the signal along the path followed to reach the regenerator.

In our OTN model, optical links are all equipped with the same type of DWDM line system, and we assume that more than one DWDM system can be installed in parallel on a link. Each DWDM line system is bidirectional, and as shown in Fig. 1, it is composed of a couple of counter-propagating fibers, the set of optical line Erbium Doped Fiber Amplifiers (EDFA), which are necessary to recover optical propagation losses, together with a wavelength multiplexer (mux) and a de-multiplexer (demux) at each terminal of the system. In this initial OTN model, we do not consider other optical-domain processing devices such as dispersion compensators, WDM-channel equalizers, etc. We assume that the wavelength muxes and demuxes of the line systems are not equipped with transponders, which as explained above, are included in the nodes. All the line systems deployed in the network have a pre-assigned fixed capacity in terms of the maximum number of

WDM channels supported—typically 40 wavelengths.

Many research works about translucent OTNs assume that all wavelength channels in a line system have the same characteristics. In this work, however, we consider a more realistic model. From a signal-propagation point of view, each wavelength channel within the set of wavelengths supported by a DWDM system (a.k.a the wavelength comb) has a different behavior in practice. As mentioned above, the quality of an optical signal is measured by the BER at the receiver. When the BER of a lightpath is over a given threshold, the connection is blocked. The BER degradation during propagation is due to the influence of both linear and non linear impairments, which are almost all wavelength dependent (especially the non-linear ones). Therefore, the degradation of the BER depends on the wavelengths assigned to a connection along its path. The fact that the BER must be below a given bound imposes a limit to the maximum distance reachable by an optical signal, which is represented by the Maximum Transmission Distance (MTD) parameter, assuming that propagation occurs under wavelength continuity and without regeneration. If we assume that translucent nodes do not degrade the BER, the MTD only depends on the characteristics of the DWDM line system, so the MTD becomes a function of the wavelength.

Figure 2 shows an example—inspired in the results found in [3]—assuming a BER threshold of  $10^{-9}$  and a DWDM comb of 40 wavelengths. Even though the values shown in Fig. 2 depend on the technical data of the specific line system used, the shape of the curve and the global behavior of the MTD as a function of the wavelength are common to most of the existing line systems—at least those equipped with EDFAs. Figure 2 shows that the maximum reach varies with the wavelength and the variations are significant (in the range from 2000 km to more than 4000 km). The figure also reflects that the best portion of the spectrum corresponds to the Erbium peak (1530-1565 nm). In order to model this behavior in a simple way, we introduce the concept of a “wavelength class”. From Fig. 2 we observe that it is possible to group the DWDM channels in classes, each with a similar MTD value for the different channels in the class. The number of wavelength classes and their upper and lower limits are a choice of the network designer. In Fig. 2 we can consider three classes: i) *Gold class*, with a MTD greater or equal than 3500 km (wavelengths from 12 to 27 in the example, 16 in total); ii) *Silver class*, with a MTD in the range of 3000 and 3500 km (wavelengths from 8 to 11 and

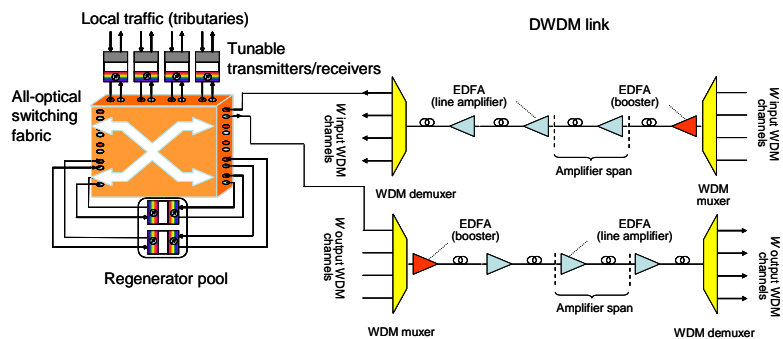


Fig. 1. Main components of the translucent OTN model.

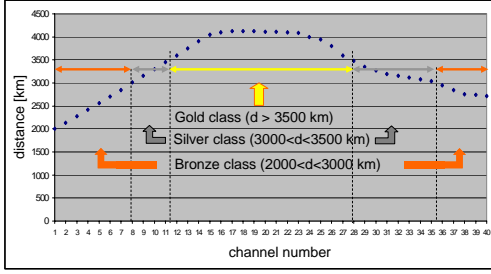


Fig. 2. Example of the MTD of the wavelengths of a 40-channel DWDM system, when the BER tolerated is  $1 \times 10^{-9}$  at the receiver.

from 28 to 35 in the example, 12 in total); iii) *Bronze class*, with a MTD in the range of 2000 and 3000 km (wavelengths from 1 to 7 and from 36 to 40 in the example, 12 in total).

Wavelength classification is introduced here with the objective of optimizing the allocation of regenerators and reducing costs. More precisely, wavelength classification can be used by the RWA process, in order to choose the WDM channel taking into account the distance that has to be covered by a given connection. In general, the Gold class should be used for longer paths and the other classes for shorter ones.

### III. ASSESSMENT OF THE OPTICAL SIGNAL DEGRADATION

In this section we introduce a straightforward methodology for assessing the physical-layer impairments along a transparent path (or sub-path). According to the network topology designed during the dimensioning phase, the connection path assigned by the routing operation, the wavelengths assigned to the connection at each line system traversed, and the placement of the regenerators, it is possible to ascertain whether the final BER at the receiver is below a specified threshold or not. To this end, an effective method for estimating the optical signal degradation along a path is required. This can be tackled by observing that the BER threshold translates by well-known relations into a threshold value of the so-called *Personick's Q factor* [4], or simply the quality factor  $Q$  [5]. The  $Q$  factor can be evaluated as a function of the transmission-system parameters and the transmission impairments. Without any error correction mechanism on the digital signal at the receiver, a quality factor  $Q = 16.9$  dB corresponds to a BER of approximately  $1 \times 10^{-12}$ . Typically, the requirements for the minimum value of  $Q$  of a signal at the receiver are about 17 dB without error correction, and 12 dB in case of error correction. The expression used for evaluating the  $Q$  factor at the endpoint of a transparent path (or sub-path) is given in (1).

$$Q_{end} = a_0 + a_1 OSNR_{end} + a_2 N_{SPAN} + a_3 (P_0 N_{SPAN})^B \quad (1)$$

According to (1) the quality factor depends both on linear and non-linear effects. The  $OSNR_{end}$  factor is the optical signal to noise ratio expressed in dB at the receiver. The terms  $a_2 N_{SPAN}$  and  $a_3 (P_0 N_{SPAN})^B$  take into account the non-linear effects, considering all amplifiers along a path (booster at the beginning of the line and line amplifiers at intermediate sites on the lines) for the translucent OTN model described in Section II.  $N_{SPAN}$  is the number of spans of the transparent path (a

span is the portion of a link between two amplifiers), and  $P_0$  [dBm] is the power level at the signal launch (typically 3 dBm). The coefficients  $a_0, a_1, a_2, a_3$ , and  $B$ , on the other hand, depend on the type of line systems used and should be tuned by an on-field measurement campaign. Typical values were suggested by the FP6 European research project NOBEL I [6]:  $a_0 \cong 0.4, a_1 \cong 1, a_2 \cong -0.04, a_3 \cong 0.02$  and  $B \cong 0.2$ .

The output lightpath (or sub-path) OSNR can be calculated considering the OSNR across each of its elementary components and then combining the partial results. We consider as elementary components all the spans and the nodes along the (sub-)path. If  $i$  indicates the generic component,  $OSNR_i$  contribution is computed as follows:

$$OSNR_i \text{ [dB]} = P_0 \text{ [dBm]} - QN - |T_i| \text{ [dB]} - F_i \text{ [dB]} \quad (2)$$

where  $QN$  is the quantum noise (typical value is -58 dB),  $F_i$  [dB] is the noise figure of the optical amplifier belonging to the component and  $T_i$  is the total attenuation of the element in dB. When  $i$  refers to a span,  $F_i$  is the noise figure of a line or a pre-amplifier (assumed to have the same characteristics); when  $i$  indicates a node,  $F_i$  is the noise figure of the booster amplifier located at the output of the node. Similarly,  $T_i$  is the attenuation of the fiber for a span, and of the switching fabric for a node. The OSNR at the end of the transparent (sub-)path is then expressed in linear units by  $R_{Total}$ , computed as follows:

$$OSNR_{end} = 10 \log_{10}(R_{Total}), \quad \text{with} \quad \frac{1}{R_{Total}} = \sum_i \left( \frac{1}{R_i} \right) \quad (3)$$

where  $R_i$  is the OSNR (in linear units) of the element  $i$  of the (sub-)path ( $R_i = 10^{OSNR_i/10}$ ). In this framework, (1) allows to estimate the end-to-end impairment of an optical connection traveling across the translucent OTN.

#### A. Assessing the Personick's Q factor along a lightpath

Let us consider Fig. 3, where 4 nodes are connected by 3 line systems. The lightpath begins in a node in Geneva, crosses Link 1 (128 Km) passing through a node in Milano, then crosses Link 2 (298 km) passing through a node in Pisa, and reaches the destination node in Rome through Link 3 (580 km). We assume that the spans of a given link are of equal length, i.e. the length of the link divided by the number of amplifiers installed in the line, considering line amplifiers plus the pre-amplifier. Notice that in practical settings the spacing between amplifiers might not necessarily be uniform. We also assume that, in each element, losses are exactly compensated by the amplifier gain. When the  $Q$  factor is evaluated on a path involving  $n$  nodes (including source and destination), only  $(n - 1)$  nodes contribute to the impairment, as the lightpath does not cross the destination node booster. In order to estimate the  $Q$  Personick factor for the lightpath between Geneva and Rome we use the set of parameters shown in Table 1 (extracted from the studies developed within the European project NOBEL I [6]). Based on these parameters, the procedure for the computation of the  $Q$  factor comprises the following three steps.

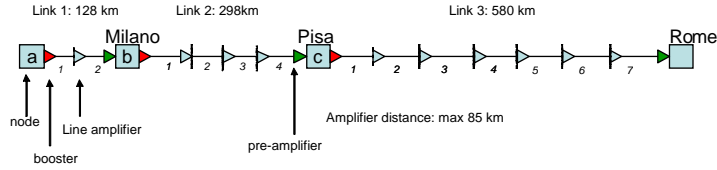


Fig. 3. Example describing the step-by-step computation of the  $Q$  factor on a three-hop lightpath.

**Step 1:** Computation of a node's OSNR—this parameter is clearly independent from the characteristics of the links. The details of its computation are shown in Table 2.

**Step 2:** Computation of the link dependent parameters (shown in Table 3).

**Step 2:** Computation of the  $Q$  factor for the overall lightpath (shown in Table 4).

As described in Section II, in a transmission system that is not perfectly compensated and/or equalized, each wavelength channel in the DWDM comb can be subject to different levels of impairment, so the  $Q$  factor estimated in Table 4 might vary depending on the wavelength chosen. The potential risks of overlooking the wavelength selection without perfect compensation shall be analyzed in Section V.

Table 1. Model parameters and values used in the example

$s_{\text{ampl}}$ : Maximum span length [km]	85
$\alpha$ : Cable attenuation [dB/km]	0.23
$CM$ : Cable margin [dB]	3
$QN$ : Quantum noise [dB]	-58
$F_L$ : Noise Figure of line ampl. and pre-ampl. [dB]	5
$F_B$ : Noise Figure of a booster [dB]	6
$P_0$ : Power level at the signal launch [dBm]	3
$T_{\text{node}}$ : Switching-fabric attenuation [dB]	13.0
$a_0$	0.4
$a_1$	0.96
$a_2$	-0.041
$a_3 = B/10$	0.02

Table 2. Computation of node parameters

$OSNR_{\text{node}}$ [dB]	$P_0 - QN - T_{\text{node}} - F_B$	42.0
$1/R_{\text{node}}$ (in linear units)	$10^{-OSNR_{\text{node}} \text{ (dB)}/10}$	6.32E-05

#### IV. UNCERTAINTIES IN THE ESTIMATION OF THE $Q$ FACTOR

There are primarily two sources of uncertainties in the estimation of the  $Q$  factor. On the one hand, the dimensioning phase of an OTN is typically performed under deterministic load conditions—using either an estimated or a measured traffic matrix. The role of the RWARP process is to determine the number of systems required in each link, and the number of regenerators to install in each translucent node, so as to route the expected traffic demand. Clearly, once the OTN is operational, the traffic load might drift from the initial estimation, which can cause that part of the lightpaths that were planned to be routed through a certain path, end up using a different path. The overall effect is that under dynamic traffic conditions, the current values of  $Q$  in the OTN might be different

Table 3. Computation of link parameters

		Length (km)		
		L1=128	L2=298	L3=580
Number of spans	$N_{\text{span}} = \left\lceil \frac{L}{s_{\text{ampl}}} \right\rceil$	2	4	7
Span length [km]	$L_{\text{span}} = L / N_{\text{span}}$	64.0	74.5	82.9
$T_{\text{span}}$ [dB]	$\alpha L_{\text{span}} + CM$	17.72	20.14	22.06
$T_{\text{span}}$ (in linear units)	$\frac{T_{\text{span}} \text{ (dB)}}{10}$	59.16	103.16	160.59
$OSNR_{\text{span}}$ [dB]	$\frac{P_0 - QN - T_{\text{span}} - F_L}{10}$	38.28	35.87 dB	33.94
$1/R_{\text{span}}$	$\frac{10^{-OSNR_{\text{span}} \text{ (dB)}/10}}{10}$	1.49E-04	2.59E-04	4.03E-04
$1/R_{\text{link}}$	$\frac{1}{N_{\text{span}} R_{\text{span}}}$	2.97E-04	1.04E-03	2.82E-03
$R_{\text{link}}$	$(1/R_{\text{link}})^{-1}$	3364.9	964.8	354.2

Table 4. Computation of the  $Q$  factor

Number of nodes $n$	Geneva, Milan, Pisa, Rome	4
Number of span	2 + 4 + 7	13
$1/R_{\text{Total}}$	$\sum_{\text{links}} \frac{1}{R_{\text{link}}} + \frac{(n-1)}{R_{\text{node}}}$	4.35E-03
$OSNR_{\text{end}}$	$10 \log_{10}(R_{\text{Total}})$	23.6
Global non-linear effects [dB]	$a_2 N_{\text{span}} + a_3 \left( \frac{P_0}{10} N_{\text{span}} \right)^B$	-0.4914
$Q$ [dB]	$a_0 + a_1 OSNR_{\text{end}} + a_2 N_{\text{span}} + a_3 \left( \frac{P_0}{10} N_{\text{span}} \right)^B$	<b>22.6</b>

from those estimated during the dimensioning phase. For example, consider the case where the occupation in the OTN is such that the establishment of a new lightpath between Geneva and Rome in Fig. 3 needs to be routed through a path longer than expected, with more hops, hence changing the value of  $Q$  estimated in Table 4. For this source of uncertainty, the RWA process can typically track and update the values of  $Q$ , so the real  $Q$  on the network and the  $Q$  factor used by the RWA process are equal, even though they differ from the  $Q$  used during the design phase, i.e.,  $Q_{\text{design}} \neq Q_{\text{real}} = Q_{\text{RWA}}$ . The second source of uncertainty is the drift suffered by the physical-layer parameters (such as those in Table 1) from their nominal values during the operation of the OTN. For this source of uncertainty, the RWA process cannot update the changes in  $Q$  accurately, so the real  $Q$  on the network differs from the  $Q$  factor used by the RWA process. When both sources of uncertainties are considered, the overall effect is that  $Q_{\text{design}} \neq Q_{\text{real}}$  and  $Q_{\text{real}} \neq Q_{\text{RWA}}$ . In this context, three different conditions can occur during the dynamic operation of a translucent OTN.

1) **Perfect Knowledge and Perfect Matching (PKPM)** is the ideal condition. The  $Q$  factor used during the design phase is equal to the real  $Q$  on the network, and it is also the same factor currently used by the RWA process:  $Q_{design} = Q_{real} = Q_{RWA}$ .

2) **Perfect Knowledge and Imperfect Matching (PKIM)** is the condition derived from the first source of uncertainty mentioned above. In this case, the network could suffer from an inadequate allocation of resources, e.g., because the design phase was done based on rather optimistic conditions:  $Q_{design} \neq Q_{real} = Q_{RWA}$ .

3) **Imperfect Knowledge and Imperfect Matching (IKIM)** is the worst condition, as it is the combined effect of both sources of uncertainties:  $Q_{design} \neq Q_{real}$  and  $Q_{real} \neq Q_{RWA}$ .

## V. PERFORMANCE EVALUATION

Our goal is to analyze the performance of a translucent OTN under the three different knowledge and matching conditions described above. We focus on the regular operation of the OTN, i.e., after the dimensioning phase has been completed.

### A. Overview of the RWA techniques

We used two different RWA techniques. The first one is deterministic, and is used both during the dimensioning phase as well as during the regular operation of the OTN. During the dimensioning phase, the more general and deterministic RWRP process [7] is used so as to minimize the number of required resources, i.e., the number of line systems and regenerators to be installed in the translucent OTN. Regeneration is needed whenever the  $Q$  factor assessed for a given lightpath is below 17 dB. During the regular operation of the OTN, the deterministic RWA process routes every connection following the shortest path and first fit wavelength assignment, minimizing at the same time the number of regenerators used by each lightpath. The threshold of 17 dB in the  $Q$  factor is then checked for every transparent path (or sub-path).

The second RWA technique used during the regular operation of the OTN is named *Predictive Routing according to the Q factor* (PR-Q), and is based on our *Prediction-Based Routing* (PBR) mechanism [8]. PR-Q is designed to counteract the negative effects derived from the uncertainties in the physical-layer information, by means of a self-learning capability. PR-Q (see Fig. 4) utilizes  $K$  pre-computed routes using the *Minimum Coincidence and Distance* (MINCOD) routing process [9]. MINCOD finds the  $K$  paths from a source to a destination node having minimum distance and less shared links. Based on this, PR-Q keeps record of the behavior of previous connection requests using a two-bit counter [8]. The  $Q$  factor is also the reference parameter for PR-Q, to decide whether a lightpath or its transparent sub-paths would satisfy the  $Q$ -threshold constraint.

### B. Simulation set up

The simulations presented here were carried out over the PAN European Network topology using two different traffic matrices: i) a uniform matrix; and ii) a polarized matrix (Year 2007), with the traffic distribution specified in [10]. Concern-

### INPUT:

**K** number of routes sorted in increasing order according to the MINCOD metric  
**i** index of the route  
**SP(i)** number of sub-paths of route  $i$   
**t** index of the sub-path  
**W(t)** number of available wavelengths sorted in decreasing order according to the  $Q$  factor in sub-path  $t$   
**j** index of a wavelength  
**Q(t, j)** the  $Q$  factor of the signal in sub-path  $t$  and wavelength  $j$   
**Qmin** minimum Quality factor required (17dB)  
**TBC(i, t, j)** two bit counter of path  $i$ , sub-path  $t$ , and wavelength  $j$

### OUTPUT:

**ROUTE** the route selected  
**{LAMBDA(t)}** set of wavelengths in each sub-path  $t$  of the route selected

```

For i = 0 to (K - 1)
  For t = 0 to (SP(i) - 1)
    Reachable = false;
    For j = 0 to (W(t) - 1)
      if (Q(t, j) >= Qmin) && TBC(i, t, j) < 2 then
        LAMBDA(t) = j;
        Reachable = true;
        break;
    if Reachable == false then break
  if Reachable == true then
    ROUTE = i;
    break;

```

Fig. 4. The PR-Q algorithm.

ing the uniform traffic matrix, the static demand, used in the dimensioning phase, consists of one bidirectional connection for each pair of nodes, which implies a total of 378 bidirectional connections for the PAN European Network. The dynamic demand in this case, consists of an offered traffic of 1 Erlang between each pair of nodes, which also corresponds to a total of 378 Erlang in the Network. The dynamic traffic is assumed to have an exponential distribution both in the inter-arrival and holding time. For the Year 2007 traffic matrix, the resource requirements are computed in terms of 10 Gbit/s channels, according to the bandwidth requirement between the nodes as specified in [10]. In this setting, the dynamic traffic reaches 517 Erlang, with a static demand, used in the dimensioning phase, of 741 10 Gbit/s channels (notice that the number of channels has to be an integer, while the traffic in Erlang units might not).

The line systems installed in the links of the network are of 40 DWDM channels at 10 Gbit/s, and multiple lines in parallel are installed where required. For the wavelength comb we considered the following two cases: i) the OTN is perfectly compensated, i.e., all wavelengths belong to a single class and can reach the same MTD; ii) the network is not perfectly compensated, and similarly to the example in Fig. 2, we use a piecewise function to group wavelengths into the following three classes according to their MTD: Gold with 20 wavelengths, Silver with 10 wavelengths, and Bronze with the remaining 10 wavelengths. This classification yields a nominal penalty of  $Q_{Silver} = 0.9 Q_{Gold}$  for the Silver class, and  $Q_{Bronze} = 0.75 Q_{Gold}$  for the Bronze class. To illustrate the consequences of these penalties, let us consider again a connection request between Geneva and Rome, assuming that the value  $Q = 22.6$  dB found in Table 4 is for the Gold class. In such a case,  $Q_{Silver} = 20.34 > 17$  dB, but  $Q_{Bronze} = 16.95$  dB  $< 17$  dB, which means that a connection request would be blocked if the wave-

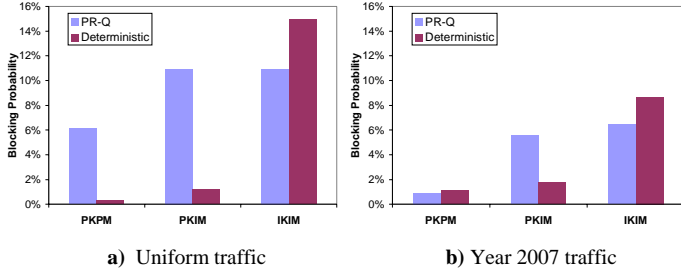


**Fig. 5.** Blocking probability for a compensated OTN (only one wavelength class exists).

length chosen belongs to the Bronze class. We have carried out the simulations for three uncertainty scenarios:

- **PKPM:** where  $Q_{design} = Q_{real} = Q_{RWA}$ .
- **PKIM:** where  $Q_{RWA} = Q_{real} = Q_{design} - 2$  dB, that is, the real  $Q$  is worsened 2 dB in order to reproduce the imperfect matching with the design conditions.
- **IKIM:** where  $Q_{real} = Q_{design} - 2$  dB and  $Q_{RWA} = Q_{design}$ . Now there is also an imperfect knowledge because  $Q_{RWA} \neq Q_{real}$ .

Figure 5 shows the blocking obtained with the two RWA techniques (deterministic and predictive PR-Q with  $K = 2$ ), under different traffic conditions, namely, uniform on the left and polarized Year 2007 on the right. Figure 5 corresponds to the case where the OTN is perfectly compensated and equalized, i.e., a single wavelength class exists, and the results are detailed for the three different knowledge and matching conditions. The first observation from Fig. 5 is that the OTN experiences blocking even under the ideal case of PKPM. This is because the dimensioning phase is typically carried out using a static traffic matrix, so the designer should over-dimension the network in order to guarantee zero blocking even in the case of PKPM. As expected, the deterministic process shows a rather low dependency on the matching condition (transition from PKPM to PKIM), but it strongly depends on the knowledge condition (transition from PKIM to IKIM). It is also important to notice that as the knowledge and matching conditions are relaxed, the blocking increases considerably, so once again, the designer should over-dimension the network in order to reach the expected blocking bound. Figure 5 also shows that the deterministic RWA technique outperforms the predictive one in case of perfect knowledge, though it performs significantly worse than the latter in the more realistic case of imperfect knowledge. This confirms the robustness of predictive RWA strategies to deal with the typical drifts and uncertainties around the physical-layer parameters. The results show that, in opposition to a deterministic RWA, PR-Q is almost insensitive to the knowledge condition.

Figure 6, on the other hand, shows the potential impact of overlooking the maximum distance reachable by the different wavelength channels when the OTN is not perfectly compensated. As in previous works, we assumed all the wavelengths with the same characteristics during the dimensioning phase, albeit they do not. The results in Fig. 6 show the consequences

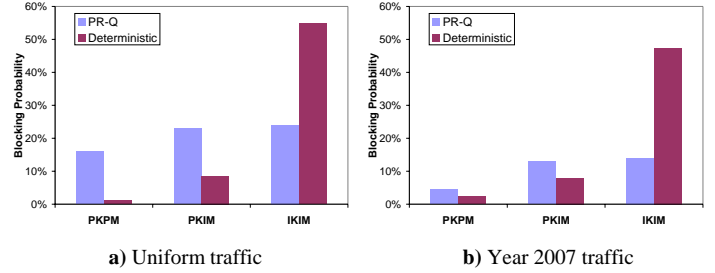


**Fig. 6.** Potential effects on the blocking when the wavelength channel assignment is overlooked in an uncompensated OTN.

on the blocking when the penalties in the  $Q$  factor described above are neglected. More specifically, by comparing the blocking in Fig. 5 and Fig. 6, it is clear that for OTNs that are not perfectly compensated, the performance experienced in practice might result significantly worse than expected.

## VI. CONCLUSION

In this paper we have investigated the performance of translucent OTNs under dynamic traffic and uncertainties in the physical-layer parameters. We introduced a new methodology for assessing the optical signal degradation along a transparent (sub-)path, and based on this, we have shown the effectiveness of predictive RWA techniques in dealing with the typical drifts and uncertainties in the physical-layer parameters. We have also analyzed the impact of overlooking the MTD reachable by the different wavelength channels when the OTN is not perfectly compensated.

For future work, we plan to extend our OTN model and assess the impact of other sources of impairment such as crosstalk, i.e., the interference between WDM channels.

## REFERENCES

- [1] Y. Pointurier et al "Analysis of Blocking Probability in Noise and Crosstalk Impaired All-Optical Networks," IEEE INFOCOM 2007, Anchorage, Alaska, USA, May 2007.
- [2] S. Pachnicke et al "Physically Constrained Routing in 10Gb/s DWDM Networks Including Fiber Non linearities and Polarization Effects," JLT vol.24 n°9 September 2006.
- [3] C. Malouin et al., "Verifying agile transparent system performance with field testing", OFC 2004.
- [4] S.D. Personick, "Receiver Design for Digital Fiber Optic Communication Systems, I", Bell Syst. Tech. J, Vol. 52, No. 6, July-August, 1973, pp. 843-874.
- [5] P. Kulkarni et al "Benefits of Q-factor based routing in WDM metro networks", ECOC 2005.
- [6] "Next Generation Optical Networks for Broadband European Leadership", www.ist-nobel.org/Nobel/servlet/Nobel.Main.
- [7] G. Maier et al, "Cross-Layer Control of Translucent Optical Networks under Physical-Parameter Uncertainty", UPC-DAC-RR-2008-52 Tech. report, Dept of Computer Architecture, UPC, 2008.
- [8] E. Marín-Tordera, X. Masip-Bruin, S. Sánchez-López, J. Solé-Pareta and Jordi-Domingo-Pascual, "The Prediction-Based Routing in Optical Transport Networks", Computer Comm. vol.29:7, April 2006.
- [9] E. Marín-Tordera et al, "MINCOD-MTD: A RWA Algorithm in Semi-Transparent Optical Networks", ECOC 2007.
- [10] Deliverable D21 of Nobel Project 2, "Preliminary Report on Multilayer Traffic Engineering and Resilience Mechanism" (A2.1 part).